HORIZON 2020

Research Infrastructures

H2020-INFRAIA-2014-2015

INFRAIA-1-2014-2015 Integrating and opening existing national and regional research infrastructures of European interest

ENSAR2

European Nuclear Science and Application Research 2

Grant Agreement Number: 654002

Deliverable 15.1

Report on the Characterization of a Niobium Disk under RF

Version: final
Author: Oleksandr Hryhorenko, David Longuevergne
Date: 13th December 2018

PROJECT AND DELIVERABLE INFORMATION SHEET

ENSAR2 Project Ref. №	654002
Project Title	European Nuclear Science and Application Research 2
Project Web Site	http://www.ensarfp7.eu/
Deliverable ID	D15.1 - TecHIBA
Deliverable Nature	Report
Deliverable Level*	PU
Contractual Date of Delivery	28th February 2019
Actual Date of Delivery	28th February 2019
EC Project Officer	Mina Koleva

* The dissemination level are indicated as follows: PU – Public, PP – Restricted to other participants (including the Commission Services), RE – Restricted to a group specified by the consortium (including the Commission Services). CO – Confidential, only for members of the consortium (including the Commission Services).

DOCUMENT CONTROL SHEET

Document	Title: Report on the Characterization of a Niobium disk under RF	
	ID: 15.1	
	Version: Final	
	Available at: http://www.ensarfp7.eu/	
	Software Tool: Microsoft Office Word 2007	
	File: ENSAR2_Deliverable_ISACA	
Authorship	Written by:	Oleksandr Hryhorenko
	Contributors:	David Longuevergne
	Reviewed by:	Matthieu Lebois
	Approved by:	

DOCUMENT STATUS SHEET

Version	Date	Status	Comments
0.0	01/08/2018	For internal review	Partial
1.0	13/12/2018	For internal review	Final
final	28/02/2019	Submitted on EC Participant Portal	
		Final version	

DOCUMENT KEYWORDS

Keywords	Mechanical polishing, superconductivity, radiofrequency (RF), superconducting cavities (SRF), surface treatment, Niobium

Disclaimer

This deliverable has been prepared by Work Package 15 (TecHIBA - Technologies for High Intensity Beams and Applications) of the Project in accordance with the Consortium Agreement and the Grant Agreement n°654002. It solely reflects the opinion of the parties to such agreements on a collective basis in the context of the Project and to the extent foreseen in such agreements.

Copyright notices

TABLE OF CONTENTS

LIST OF FIGURES

REFERENCES AND APPLICABLE DOCUMENTS

LIST OF ACRONYMS AND ABBREVIATIONS

ISACA	Improvement of Superconducting Accelerating Cavities
SRF	Superconducting Radio-Frequency
Nb	Niobium
IPNO	Institut de Physique Nucléaire d'Orsay
MP	Metallographic flat Polishing
BCP	Buffered Chemical Polishing
EP	Electro-polishing
RCD	Rigid Composite Disk
DIC	Differential Interference Contrast
SLAC	Stanford Linear Accelerator Center
CMP	Chemical Mechanical Polishing

EXECUTIVE SUMMARY

ISACA ambitions are to improve the performance and the cost effectiveness of superconducting radio-frequency (SRF) cavities production (for future projects as ILC, FCC…) by replacing or limiting the standard chemical treatment by mechanical polishing. The influence of surface quality is of paramount importance for RF characteristics and well-studied for the bulk Niobium (Nb) cavities. This deliverable 15.1 consists in the surface preparation of a Nb disk by metallographic flat polishing (MP) technique with the following cryogenic RF characterization. Polishing procedures were carried out at IPNO and the RF test at cryogenic temperature has been delayed due to unavailability of the IPNO test bench. An alternative solution but not optimal has been found at SLAC where a sample test cavity is operating.

INTRODUCTION

In SRF cavities, the internal surface is exposed to extremely high electric (up to 50 MV/m) and magnetic fields (up to 200 mT). When the electromagnetic fields approach these values, the current density can reach up to 10^{12} A/m^2 over a very thin layer of hundreds of nanometers. Consequently, any surface defect (roughness profile, pollution, deformation of crystallographic lattice) will degrade the superconducting properties. In order to avoid this negative impact on cavity performance, the damaged layer (~ 100-200 µm), caused by Nb sheet fabrication and cavity forming, has to be removed to recover a clean and damaged-free surface. This layer is typically etched by chemical polishing, as buffered chemical polishing (BCP) and electro-polishing (EP). These chemical treatments, involving extremely hazardous acids are not optimal safety-wise and quality-wise. Mechanical polishing could be a very interesting alternative as this process does not involve any acids and could achieve surface roughness one order of magnitude better than chemical processes. However, the main drawbacks are the surface pollution by embedded abrasives and the geometric limitations (mechanical polishing is optimal only on flat surfaces and not on complex geometries like accelerating cavities).

So as to keep it competitive, the mechanical polishing process has to be limited in the number of steps. Metallographic techniques usually require 5 steps to obtain optimal surfaces but this would be too expensive and too time-consuming for an industrial process. We proposed a two-step process giving very encouraging results.

- The first step, called the abrasion step, aims at removing a layer of approximately 150 microns in a reasonable time without damaging and polluting too much the surface.
- The second step, called polishing step, aims at decreasing the surface roughness down to nanometric scale and at removing the surface pollution created by the abrasion step

Optical characterizations are required to characterize and show a non-polluted and non-damaged surface. Optical characterizations are necessary but not sufficient. Not only the quality of the surface is important, but also the material quality over a depth of several hundreds of nanometers. Thus, the ultimate surface characterization testifying of the quality of the polishing procedure is the test of an RF disk at cryogenic temperature.

A. RF DISK PREPARATION

Polishing was performed on a metallographic machine (MasterLAM 1.0, LAMPLAN, Gaillard, France) shown in Fig.1. In the beginning of the study the polishing procedure was optimized on small flat Nb specimens (40 mm*10 mm). The recipe has been transferred on flat polycrystalline Nb disk of 126 mm diameter, but with some modifications. A qualitative comparison of non-polished and mirror like finished surfaces is given in Fig. 2. As the size of the polished surface is significantly increased, the device was used in oscillating mode. This feature allows the sample holder to oscillate with constant amplitude and frequency over the rotating polishing disk. The use of

this mode allows to achieve a uniform surface quality on the whole RF surface. The rotational speeds of the sample holder and the polishing disk were 300 and 150 RPM respectively. Both were turning in the same direction. The process of disk polishing consists in 2 steps of treatment.

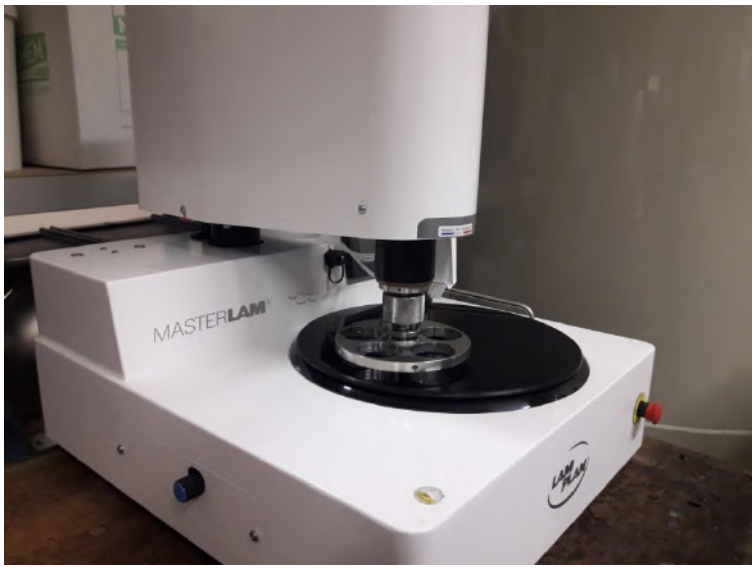

Figure 1: Metallographic polishing (MP) device.

The first step called the abrasion step aims at ensuring the planarization of the surface and at removing the polluted and damaged layer (crystalline defects). In our case, taking into consideration all the requirements, a rigid composite disk (RCD), based on Copper carrier, with a liquid suspension of diamond (3 microns) has been chosen as the first step. During the process, the abrasives behave as small “knifes” removing the material from the raw surface. However, the diamonds tend to stay embedded in the surface after abrasion and an amorphous structure is created. The first step is carried out until the planarization is reached and damages are uniformly distributed.

To remove all these embedded particles and to reveal the true structure of Nb, a chemical-mechanical action with a colloidal silica (SiO_2) solution is required. Whatever the duration of this second step, and so as to ensure a very efficient depollution of the embedded abrasives, it has been observed that the polishing step has to be interrupted every 15 minutes by a rinsing step. The device is kept running while the colloidal solution is replaced by de-ionized water and the polishing cloth is brushed to remove all the residual diamond abrasives.

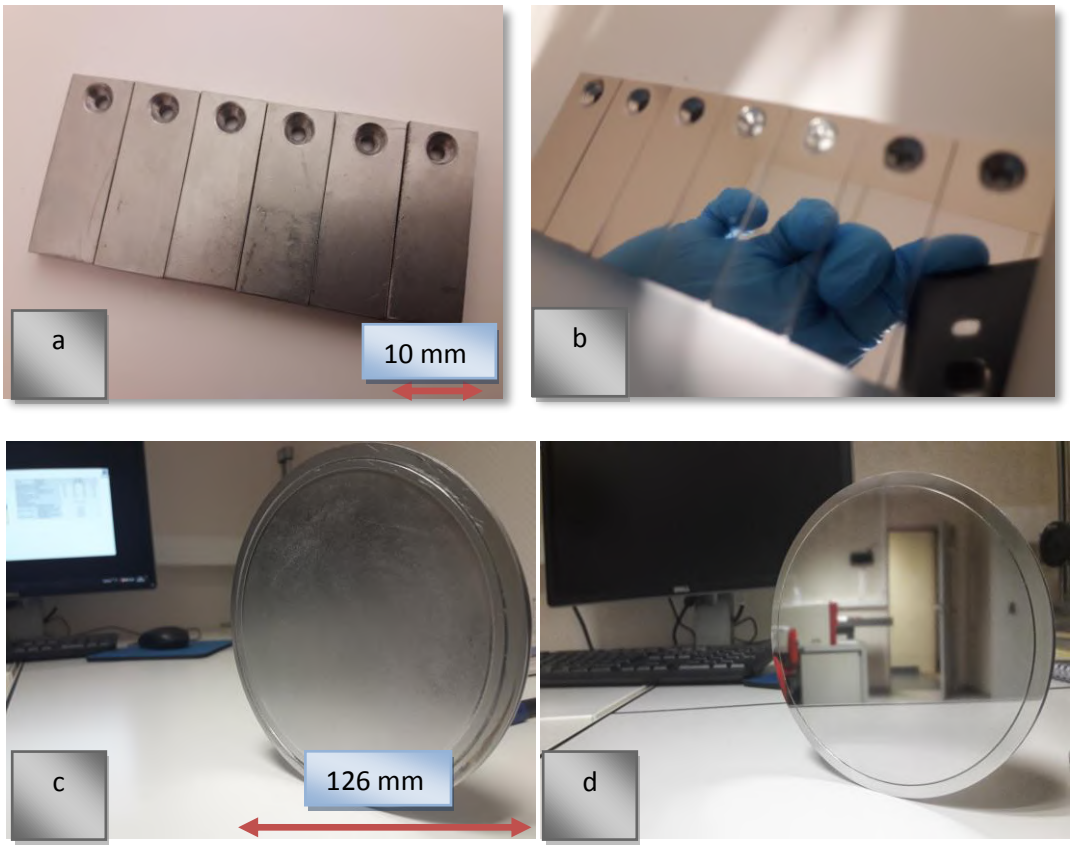

Figure 2: a) Raw Nb specimens, b) mirror finish samples after 2 polishing steps; c) non-treated Nb disk, d) mirror like finished Nb disk after 2 polishing steps.

At the end of the polishing process, the disk is taken out of machine. It is then rinsed in water, degreased with ethanol, cleaned in ultrasonic bath (of de-ionized water) and dried with Nitrogen gas.

B. Optical characterization of RF disk

Abrasion step

After abrasion step and based on the weight measurements before/after polishing the etching rate has been defined. We can distinguish 2 phases of abrasion: 1) – standard abrasion (applied pressure 22.5 kPa), 2) "gentle" abrasion (7.5 kPa). During "gentle" abrasion the applied pressure was reduced by factor 3 in order to decrease the size of artifacts (pull-outs, scratches…) inside of the Nb bulk. The etching rate depends on the applied pressure, that's why it was eventually reduced from **0.6 $\pm$ 0.06 µm/min** (standard abrasion) to **0.4 $\pm$ 0.06 µm/min** ("gentle" abrasion). **Total removed layer during abrasion was 75 $\pm$ 1 µm corresponding to 135 min of polishing.**

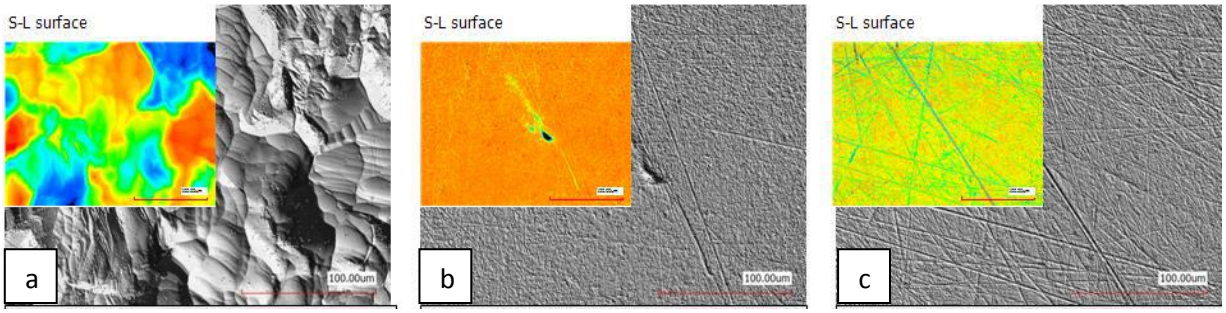

Figure 3: Laser confocal images of Nb disk in differential interference contrast (DIC) mode and height mode (S-L surface, blue color corresponds to valley region and red to hill) from left to right:
a - primary state (after some chemical polishing, BCP), b – after standard abrasion (120 minutes),
c – after "gentle" abrasion (15 minutes).

The surface roughness was measured with a laser confocal microscope Keyence VK-X 200, shown in Fig.3. The surface roughness Sa (average deviation of the surface), and the maximum height Sz (difference between highest peak and lowest pit, Sz) were used to monitor the evolution of surface roughness during the abrasion process. Table 1 presents the surface roughness parameters obtained from different locations (average of 10 measurements).

Surface roughness parameters	Sa, µm	Sz, µm
Before abrasion	1.19 ± 0.19	10.02 ± 2.75
After abrasion	0.068 ± 0.008	3.27 ± 1.09

Table 1: The initial and final values of the average surface roughness and maximum height of surface profile after abrasion step.

POLISHING STEP

During the polishing step with colloidal silica on microporous polyurethane disk, presented in later Figure 6 (a, b), the polishing parameters have been reduced as the polishing device was not powerful enough to apply the same pressure and speed parameters on such a big surface. The applied pressure was reduced from 22.5 kPa up to 7.5 kPa. We observed the formation of "bright" and "dark" spots on the disk. Figure 4 shows these regions, "bright" spots correspond to significant higher polluted regions compared to "dark" spots. Such a non-uniform surface quality is explained by a very bad distribution of the solution between the polishing cloth and the Nb disk. So as to ensure the uniformity of the polishing step, the polishing cloth (plain cloth) was replaced by a meshed cloth, shown in Figure 5 (a, b). As a result, the applied pressure on the disk could have been increased back to a normal value (22.5 kPa) and a very homogeneous surface quality has been achieved.

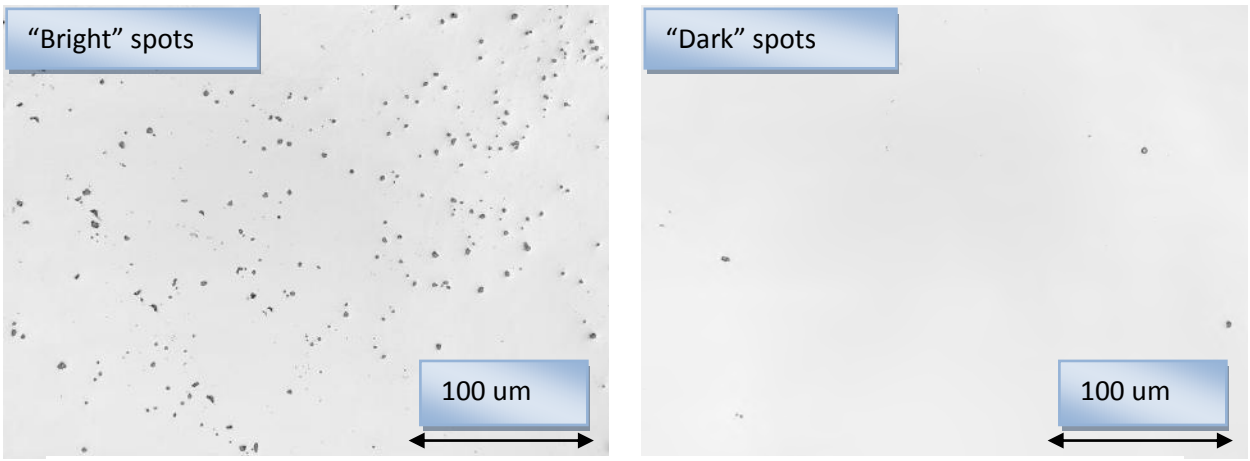

Figure 4: Laser confocal images of bright and dark region after polishing with SiO_2 during 120 minutes.

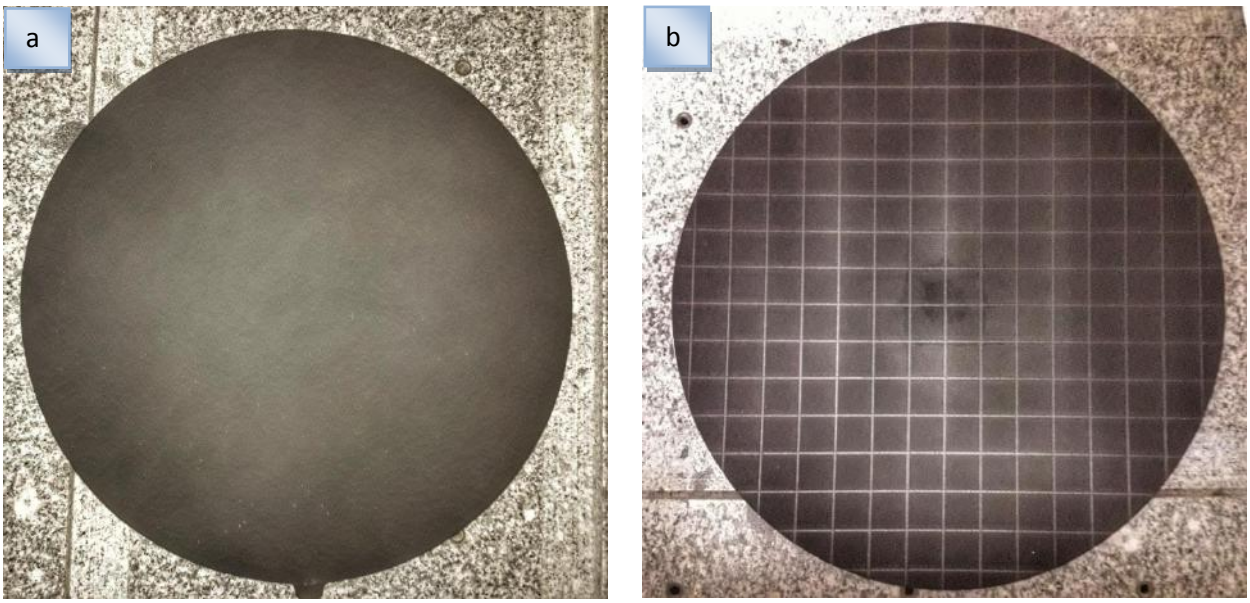

Fig. 5: 300 mm-diameter polishing cloth used for polishing step a) plain; and b) meshed.

The evolution of embedded particles as a function of time has been investigated during final polishing step on this disk. Standard ISO 25178, in particular the root square gradient (Sdq) parameter, might be used to identify the level of pollution. Sdq is calculated as a root mean square of slopes at all points and it corresponds to ratio of embedded particles to planar surface. Figure 6 shows the change of Sa (surface roughness) and Sdq parameters of the RF disk surface during the two-step polishing process. The process of grain revealing with chemical-mechanical polishing is presented in Figure 7.

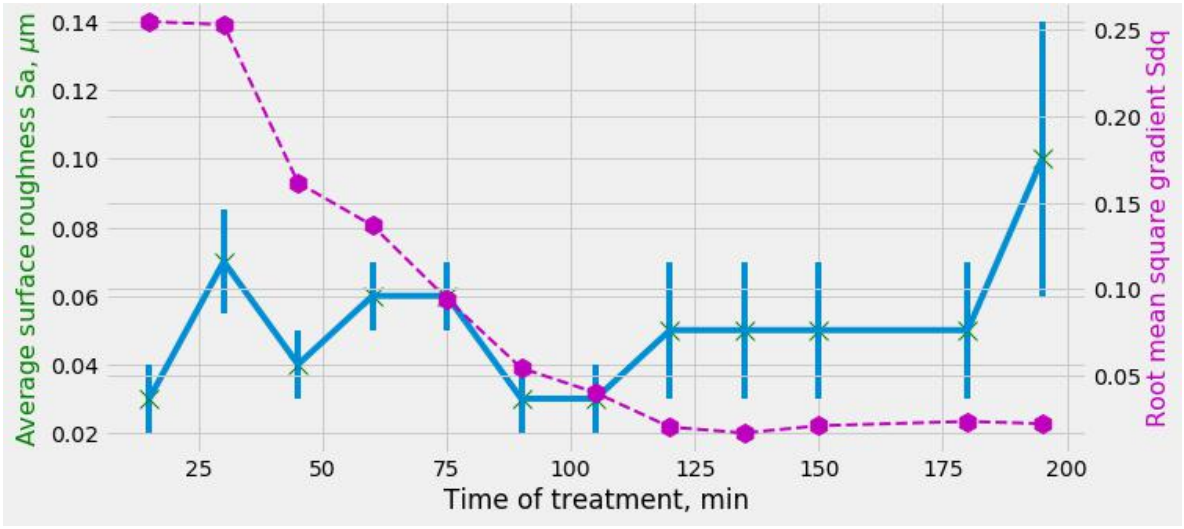

Figure 6: The evolution of surface quality as a function of time.

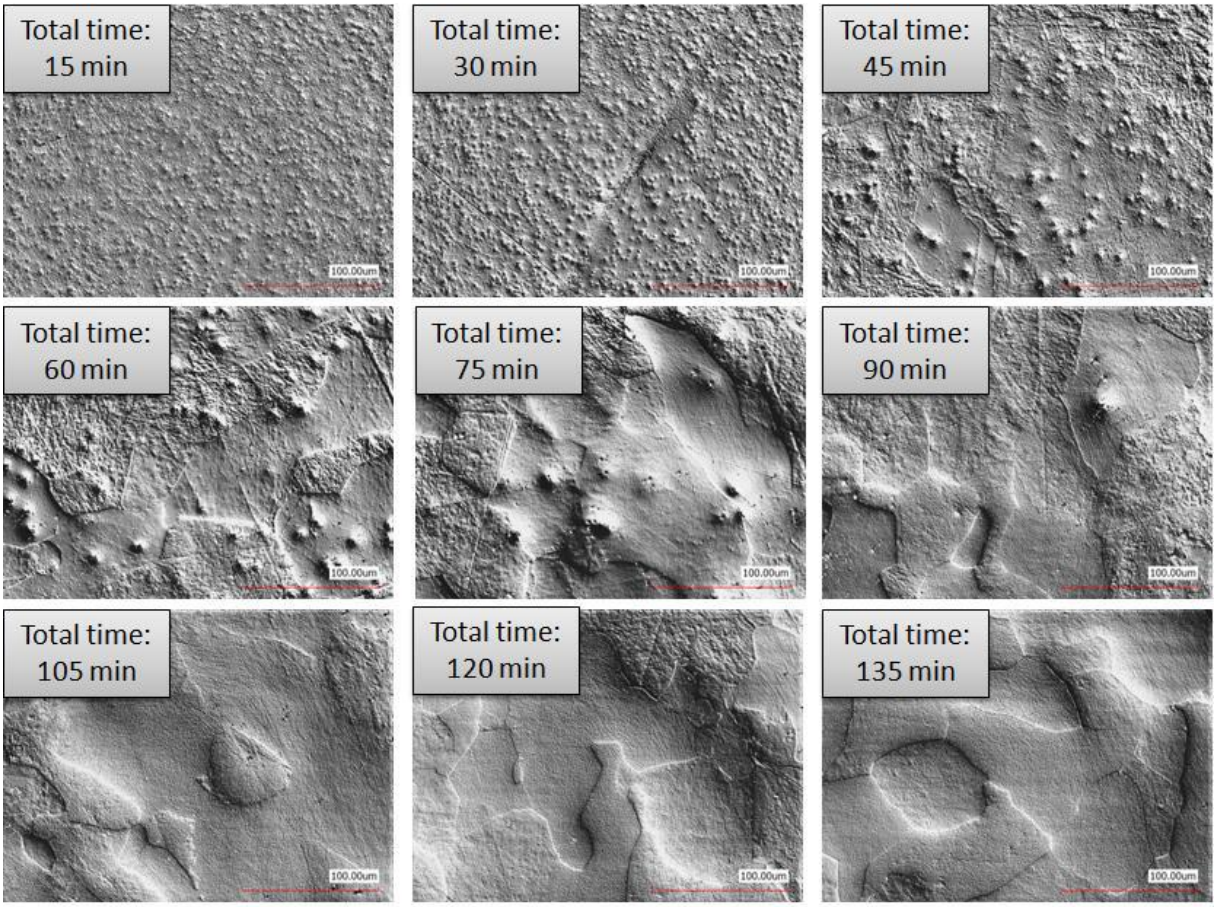

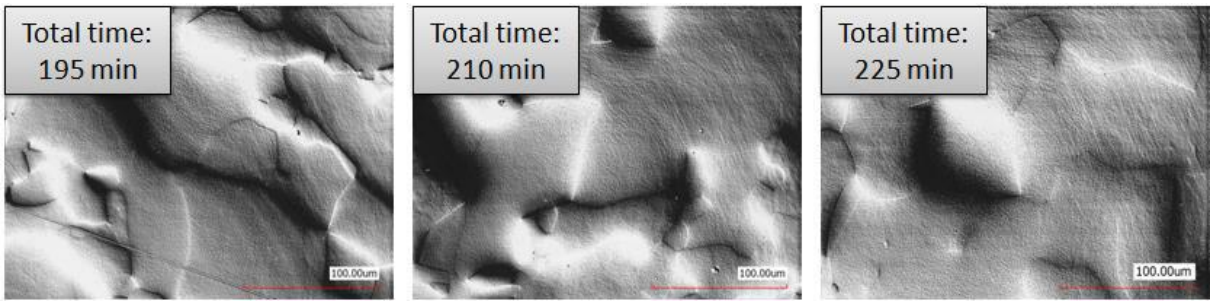

Figure 7: DIC images of surface state in different periods of time. Note: This figure shows also the evolution of embedded particles and grain formation with time.

C. RF TEST

RF measurements have been performed at SLAC (Stanford Linear Accelerator Center) in Menlo Park, California, by P. Welander. The test bench (See the Fig.8) is a hemispherical cavity which operates in pulse mode at a high frequency (11.4 GHz) and at cryogenic temperatures (typically between 15K and 3.8K). The cavity walls are made of bulk copper sputtered with Niobium on the RF side (the cavity is thus superconducting below 9.2K). This system gives the possibility to mount flat disks made of superconducting material with a diameter of 50.8±0.3 mm and with the follow thicknesses: 0.43, 1.07, 1.78, 2.44, 3.00, 5.00 and 6.35 mm.

Two samples with final thicknesses of 3.00±0.1 mm were prepared and treated at IPNO with 2-steps chemical mechanical polishing recipe (CMP) as presented previously and with the standard chemical etching (BCP) reference sample used as a reference.

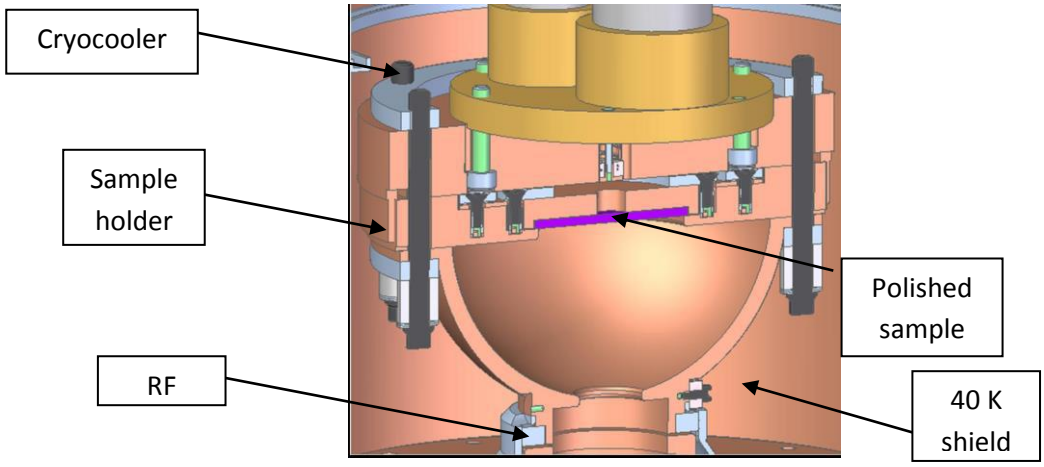

Figure 8: Design of the hemispherical cavity at SLAC.

Figure 9 shows the simulation of the magnetic field distribution on the sample with the zeros of the magnetic field in the center and on the edges of the sample. All surface H-fields are radial on the sample, so surface currents are azimuthal and with zero electrical fields on the sample. The cavity operates at the TE_{032} mode.

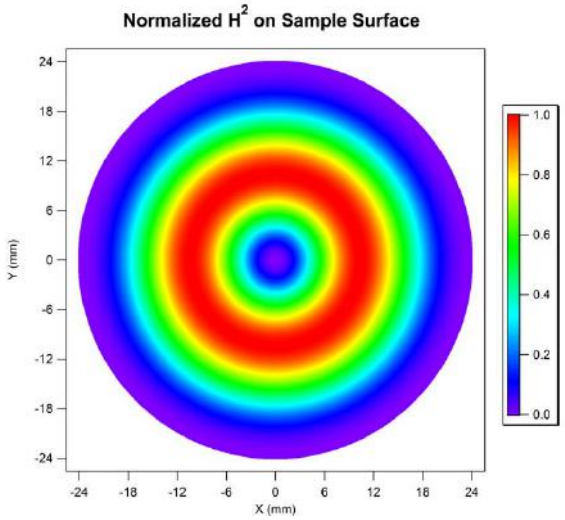

Figure 9: Simulations of the magnetic field on the sample (courtesy of P. Welander).

The measured parameter during the experiment at several temperatures is the quality factor of the resonating cavity (i.e cavity + disk). The quality factor is defined as a ratio of the total stored energy (U) and the dissipated power in the cavity (P). In the case where the surface resistance does not depend on the RF amplitude and is assumed homogeneous on the cavity and the sample, the formula is simplified and can be expressed as the ratio of a geometrical factor (G_{total}) and the surface resistances R_{disk} and R_{cavity}:

$$Q_0 = \frac{2\pi f U}{P}\frac{G_{total}}{R_s} = \frac{G_{total}}{\alpha_{disk}R_{disk} + \alpha_{cavity}R_{cavity}} \quad (1)$$

Where f is the RF frequency of the cavity, G_{total} is the geometrical factor of the resonating cavity which equals to 1403Ω and $\alpha_{disk} = \frac{G_{disk}}{G_{total}} = 0.33, \alpha_{cavity} = \frac{G_{cavity}}{G_{total}} = 0.67$. The surface resistance of the disk can be thus easily extracted from the measured Q_0.

During the experiment, the quality factor of the cavity is measured continuously while cooling down to 3.8K. The quality factors of 3 samples (BCP, CMP and SLAC reference) are shown in Fig. 10. The brown curve corresponds to a SLAC reference sample with the highest quality factor obtained, the blue curve to IPNO reference sample (BCP) and the red curve to the CMP polished sample. At critical temperature T_c (9.2K) the Niobium material has its transition from normal state to the superconducting state, which is characterized by the significant increase of the quality factor. This transition temperature could be reduced in the case of a heavily polluted surface with non-superconducting materials. The CMP sample shows the same transition temperature indicating a very limited surface pollution.

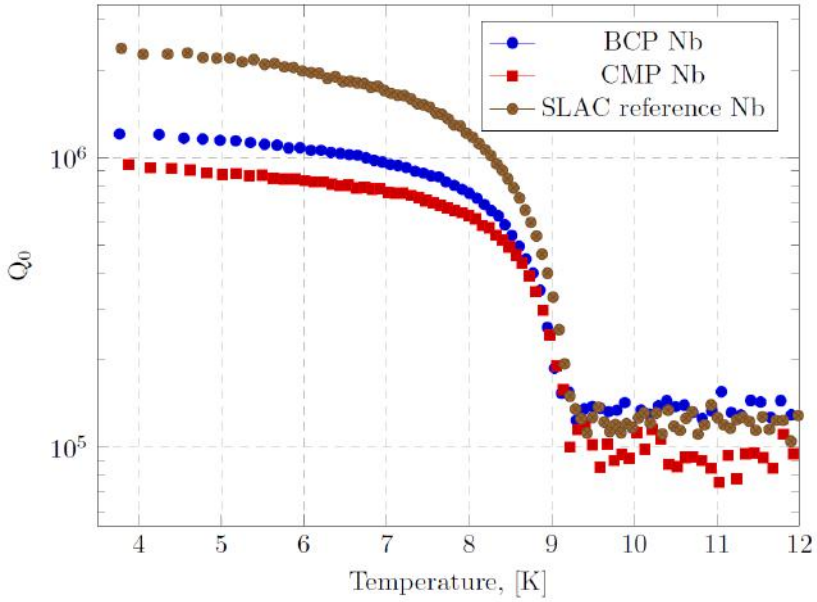

Figure 10: Dependence of quality factor as a function of temperature.

To extract the surface resistance from Figure 10, a strong assumption has to be made: the surface resistance of the reference disk is the same as the cavity. Equation1 could be then simplified as:

$$Q_{disk}=\frac{G_{total}}{R_s}=\frac{G_{total}}{\alpha_{disk}Q_{disk}}-\frac{G_{total}\alpha_{cavity}}{\alpha_{disk}Q_{ref}} \quad (2)$$

Where Q_{disk} is the quality factor of the CMP or the BCP treated sample and Q_{ref} is the quality factor of the SLAC sample.

Figure 11 shows the behavior of the extracted surface resistance as a function of the ratio T_c/T. The observed surface resistance R_s consists of the sum of the theoretical resistance predicted by the BCS model (R_{BCS}) and the residual resistance (R_{res}) defined as the surface resistance at zero Kelvin (due to the presence of normal conducting elements, oxides, hydrogen, trapped magnetic field, …)

For Niobium R_{BCS} would be typically expressed as :

$$R_{BCS}=\frac{9*10^{-5}}{T}f^2 exp\left(-\frac{1.83T_c}{T}\right) \quad \text{for T<Tc/2} \quad (4)$$

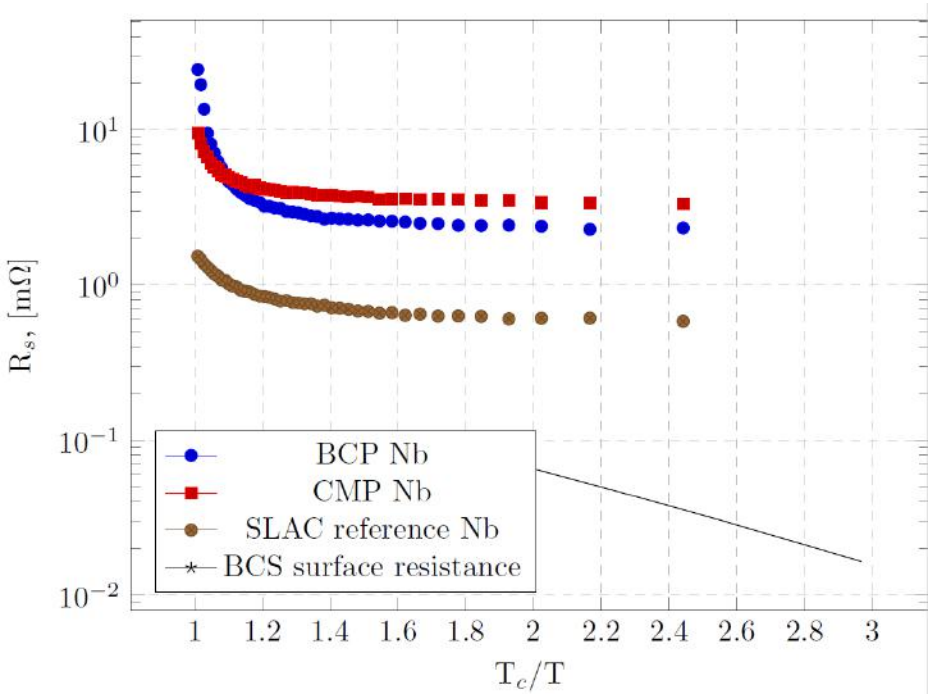

Figure 11: Surface resistance of the three sample versus T_c/T.

As shown in the Fig.11 the BCS model predicts a surface resistance well below and linearly decaying with T_c/T. Whereas all tested samples, even SLAC reference shows a very early saturation of the surface resistance corresponding to the residual resistance. These early stabilizations of the surface resistance could be the sign of systematic limitations as bad RF contacts, magnetic field trapping or pollution of the sputtered cavity itself. Moreover, the exact dimensions of SLAC reference disk could be different from our similar samples (CMP and BCP). This difference could lead to varying RF contacts explaining the change of saturation level of the surface resistance. Our both samples are very similar in dimensions and show very close results indicating a satisfying but still not optimal CMP treatment.

CONCLUSIONS AND PERSPECTIVES

A two-step polishing procedure was successfully developed at IPNO and applied on RF disk. Optical characterizations have been performed showing a non-polluted and non-damaged surface. Not only the quality of the surface is important, but also the material quality over a depth of several hundreds of nanometers. As a consequence, optical quality is necessary but not sufficient. Thus, the ultimate surface characterization testifying of the quality of this polishing procedure is the RF test at cryogenic temperature. This test performed at SLAC showed very promising results (visible superconducting transition at 9.2K). Unfortunately, because of technical limitations inducing a very early saturation of the surface resistance, the decay of superconducting BCS resistance with Tc/T couldn't be measured properly. A way to mitigate these "high frequency" limitations would be to test a sample at a lower frequency, as on IPNO test bench as soon as this one would be available (the sample disk is ready to be tested). This will definitely happen before the final report of this task.

ACKNOWLEDGEMENT

The author would like to thank the great work of SUPRATECH team for the high quality work performed for surface preparation of reference samples. Moreover, we would like to thank Paul Welander working in the Accelerator Technology Research Department from SLAC for the RF test of our prepared samples allowing us to have RF results ready for this deliverable.